Electronic Supplementary Material (ESI) for Environmental Science: Processes & Impacts.

Supporting information

Stereoisomer Specific Reaction of Hexabromocyclododecane with Fe(II) Associated with Iron Oxides

Xianmiao Zhang[a], Kristian K. Roopnarine [b], Shirley Dong [b], Urs Jans*[,a,b]

[a] Chemistry Program, The Graduate Center of the City University of New York, New York, NY, 10016, United States

[b] Department of Chemistry and Biochemistry, The City College of New York, CUNY, New York, NY 10031, United States

* Corresponding author

Mailing address: Department of Chemistry and Biochemistry, The City College of New York, 160 Convent Avenue, New York, NY, 10031.

Tel: (212) 650-8369. Fax: (212) 650-6107. Email: ujans@ccny.cuny.edu.

(A)

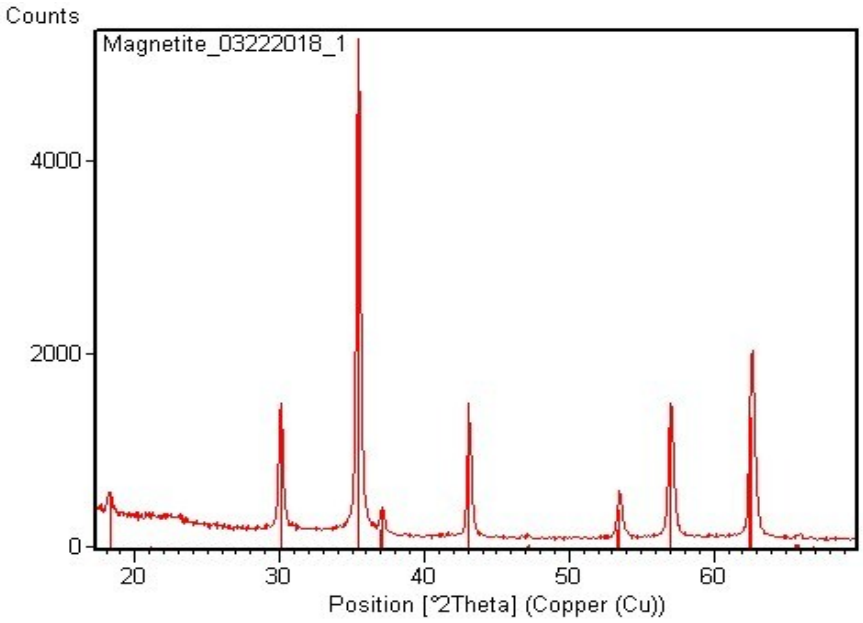
Counts
Magnetite_03222018_1
4000
2000
0
20
30
40
50
60
Position [°2Theta] (Copper (Cu))

(B)

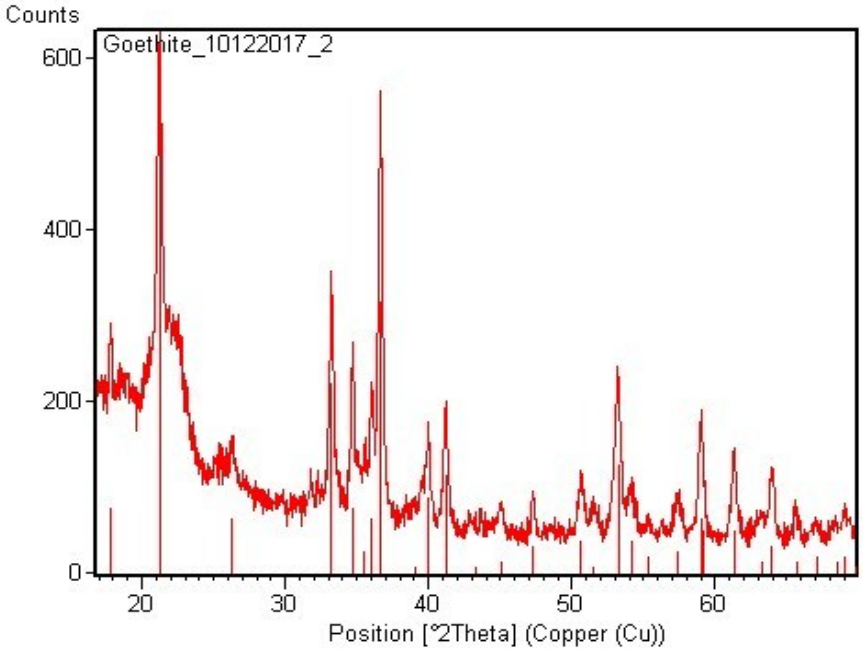
Counts
Goethite_10122017_2
600
400
200
0
20
30
40
50
60
Position [°2Theta] (Copper (Cu))

(C)

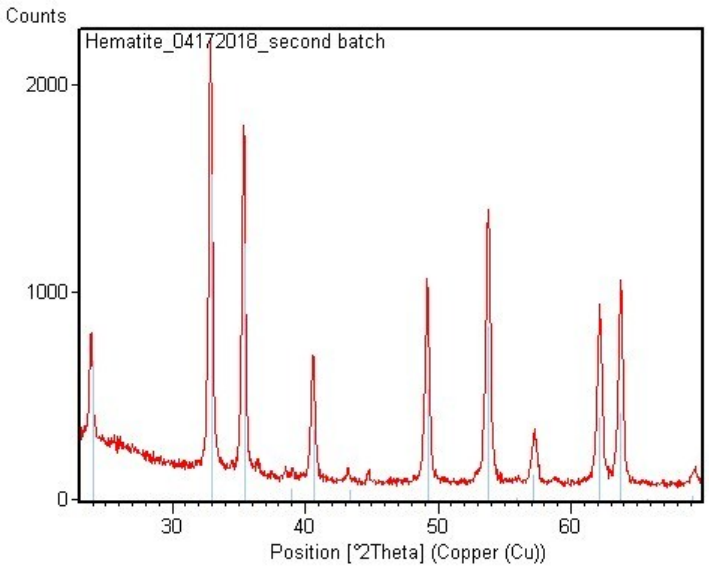

Fig. S1. XRD patterns for synthesized (A) magnetite; (B) goethite and (C) hematite.

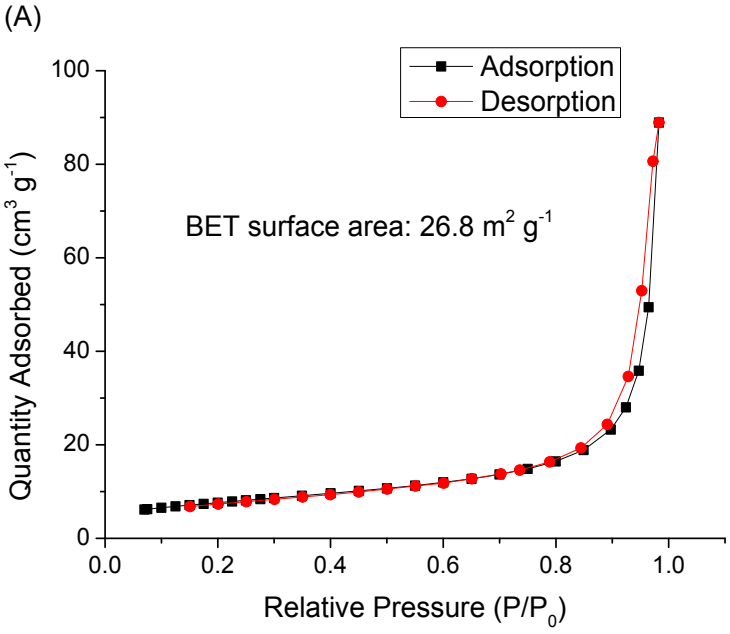

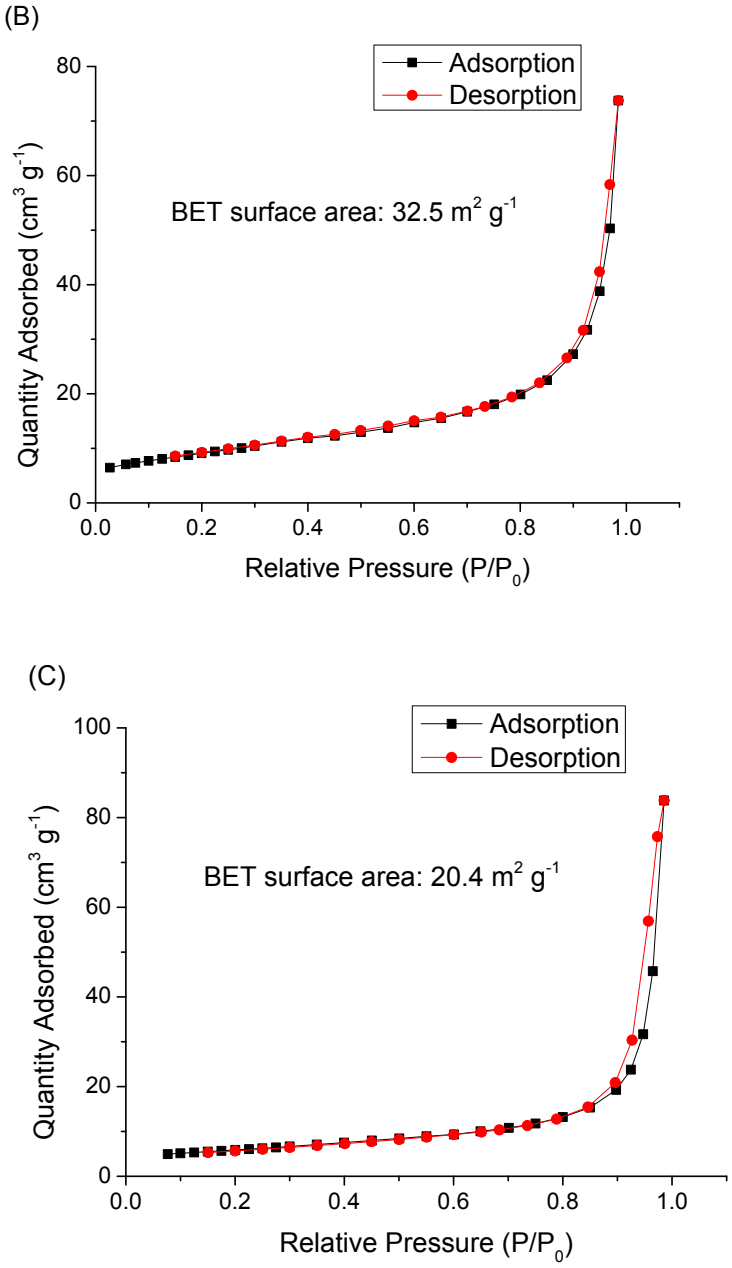

Fig. S2. Adsorption and desorption isotherms of synthesized (A) magnetite; (B) goethite and (C) hematite.

All isotherms present a typical type III behavior showing only pronounced gas uptake at high relative pressure (0.8<P/Po<1). This characteristic suggests the presence of macropores (Sing, 1982). The lack of substantial increment in adsorption quantity at low relative pressure and the missing of hysteresis loops in intermediate relative pressure indicate no micropores and mesopores were detected (Sing, 1982). Taking together, the nitrogen physisorption tests clearly display that the synthesized materials do not contain a large amount of small pores. The macropores could be ascribed to inter-particle gap or cavities.

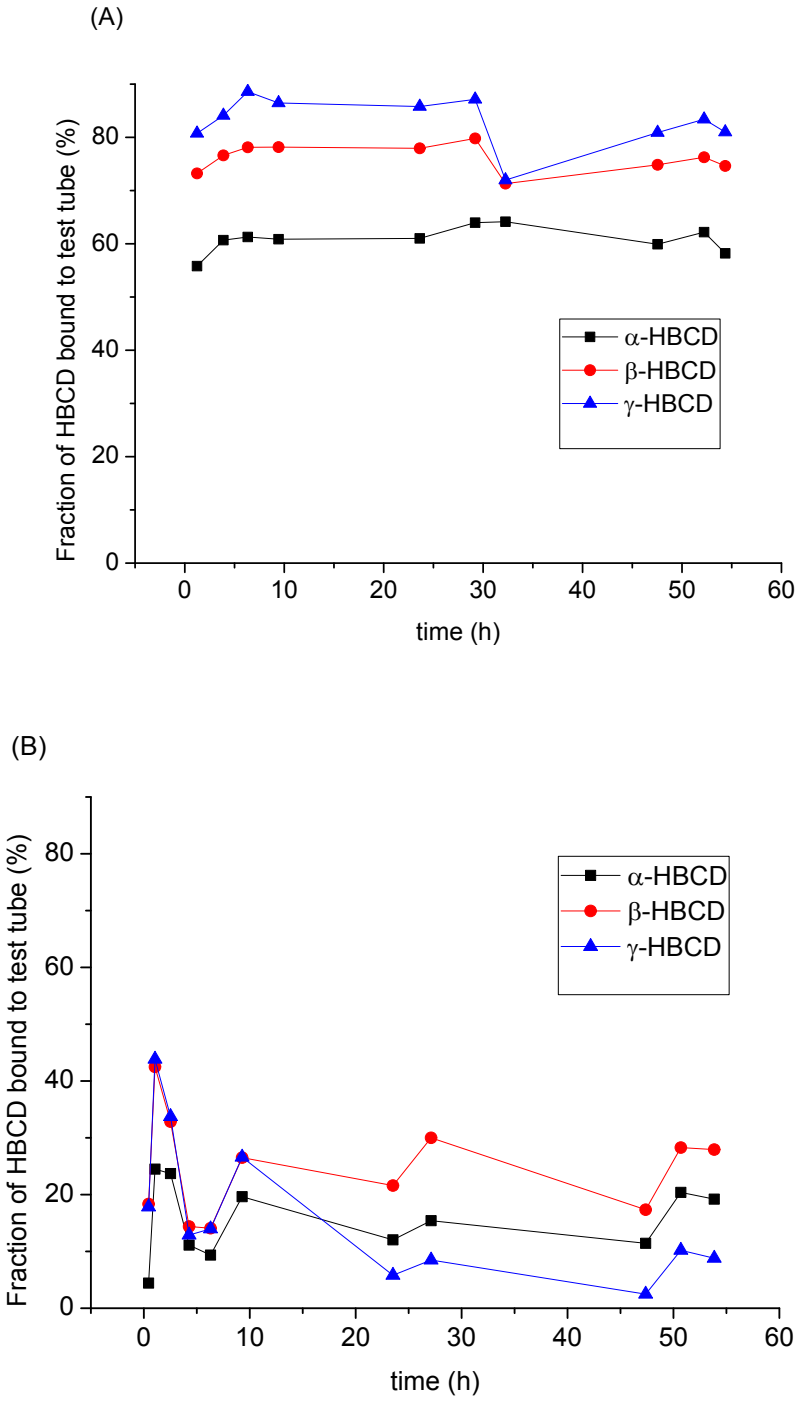

Fig. S3. Time course for the fraction of HBCD isomers bound onto the test tube surface (A) in the absence of iron oxides and (B) in the presence of 5 mg mL^{-1} goethite with 1.0 μM HBCD at pH 7.2.

(A)

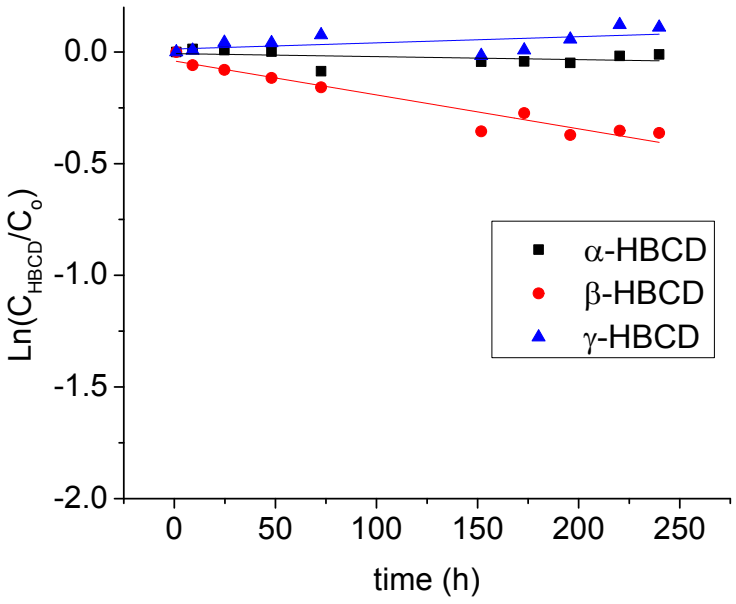
0.0
-0.5
-1.0
-1.5
-2.0
Ln(C_HBCD/C_o)
0
50
100
150
200
250
time (h)
α-HBCD
β-HBCD
γ-HBCD

(B)

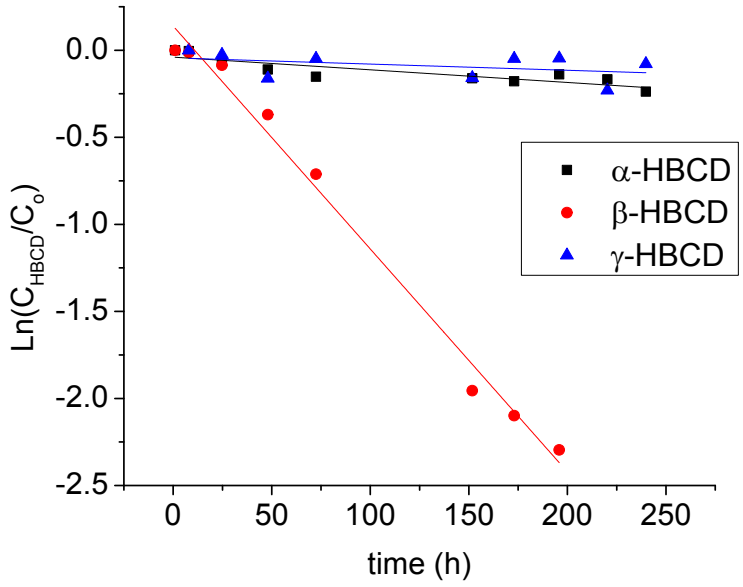
0.0
-0.5
-1.0
-1.5
-2.0
-2.5
Ln(C_HBCD/C_o)
0
50
100
150
200
250
time (h)
α-HBCD
β-HBCD
γ-HBCD

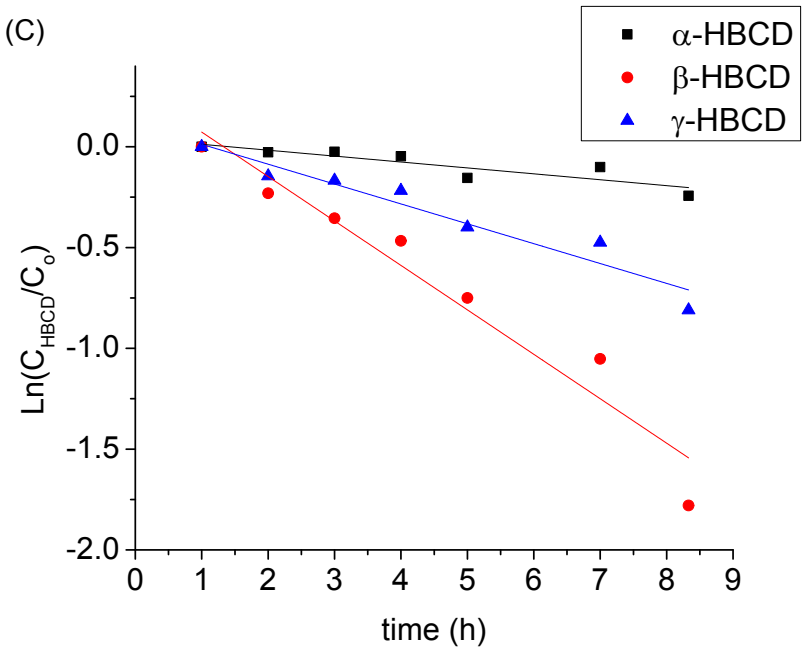

Fig. S4. Plot of $Ln(C_{HBCD}/C_0)$ versus time for the reaction of 1.0 µM HBCD in the presence of 2.5 mg mL^{-1} magnetite and an initial concentration of 6.0 mM Fe(II) at (A) pH 6.15; (B) pH 6.78; and (C) pH 6.98.

Table S1. The concentration of sorbed Fe(II) and observed pseudo-first-order rate constants for the reaction of 1.0 μM HBCD in the presence of 2.5 mg mL^{-1} magnetite and an initial concentration of 6.0 mM Fe(II) at various pH values

pH	7.17			6.98			6.78			6.15		
$Fe(II)_{sorbed}$ (mmol g^{-1})	1.24			1.20			1.03			0.84		
k_{obs} (h^{-1})	**total**	aqueous	solid	**total**	aqueous	solid	**total**	aqueous	solid	**total**	aqueous	solid
α-HBCD	**5.2(±2.1) ×10^{-2}**	1.1(±1.0) ×10^{-2}	6.7(±1.7) ×10^{-2}	**2.9(±1.7) ×10^{-2}**	NA	3.9(±1.1) ×10^{-2}	**7.3(±3.3) ×10^{-4}**	NA	8.9(±2.7) ×10^{-4}	**NA**	NA	NA
β-HBCD	**2.6(±0.5) ×10^{-1}**	3.3(±0.5) ×10^{-1}	2.5(±0.3) ×10^{-1}	**2.2(±0.6) ×10^{-1}**	2.5(±0.3) ×10^{-1}	2.2(±0.4) ×10^{-1}	**1.3(±0.1) ×10^{-2}**	1.3(±0.2) ×10^{-2}	1.2(±0.1) ×10^{-2}	**1.5(±0.3) ×10^{-3}**	NA	1.8(±0.4) ×10^{-3}
γ-HBCD	**1.5(±0.2) ×10^{-1}**	2.2(±0.5) ×10^{-1}	1.3(±0.1) ×10^{-1}	**9.9(±3.0) ×10^{-2}**	1.9(±0.4) ×10^{-1}	9.2(±1.8) ×10^{-2}	**NA**	1.8(±1.7) ×10^{-3}	**NA**	**NA**	NA	NA

The uncertainties reflect the 95% confidence limit and it is reported as $t_{95\%}$ (t-value for 95% confidence limit) times standard deviation of slope in observed pseudo-first-order rate constant determination plot.
NA = Not Available, NA is presented in the table because the reactions are too slow and k_{obs} are smaller than their uncertainties.

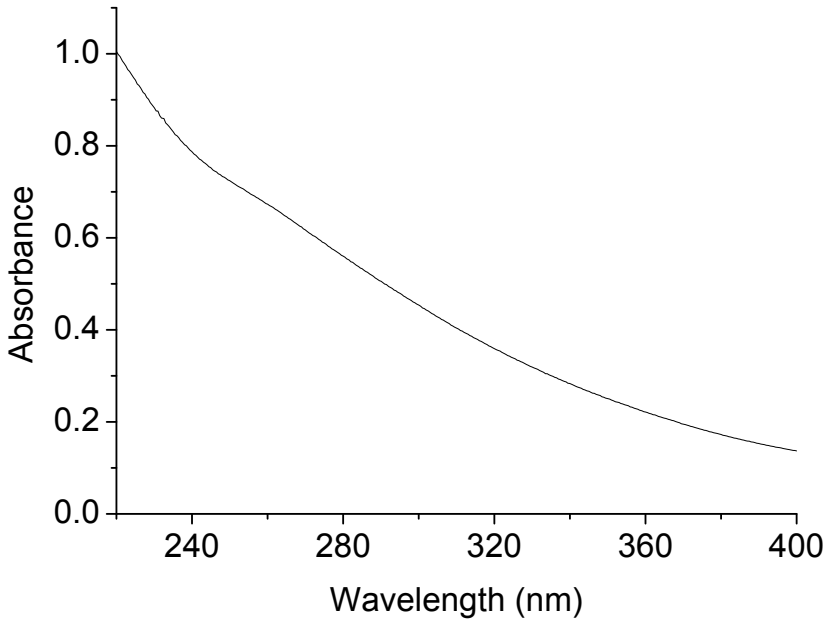

Fig. S5. UV-Vis spectrum of PPHA stock solution.

(A)

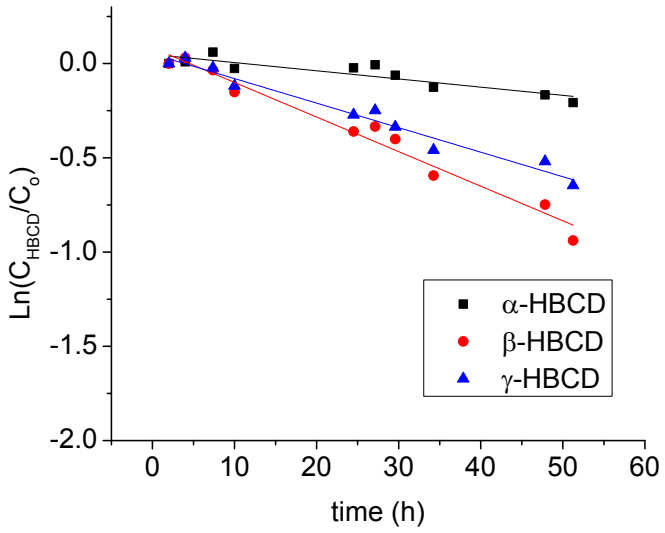
0.0
-0.5
-1.0
-1.5
-2.0
Ln(C_HBCD/C_o)
0
10
20
30
40
50
60
time (h)
α-HBCD
β-HBCD
γ-HBCD

(B)

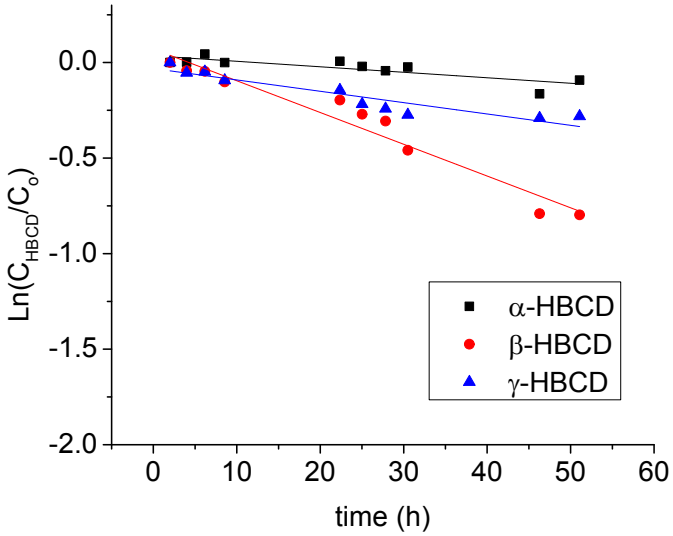
0.0
-0.5
-1.0
-1.5
-2.0
Ln(C_HBCD/C_o)
0
10
20
30
40
50
60
time (h)
α-HBCD
β-HBCD
γ-HBCD

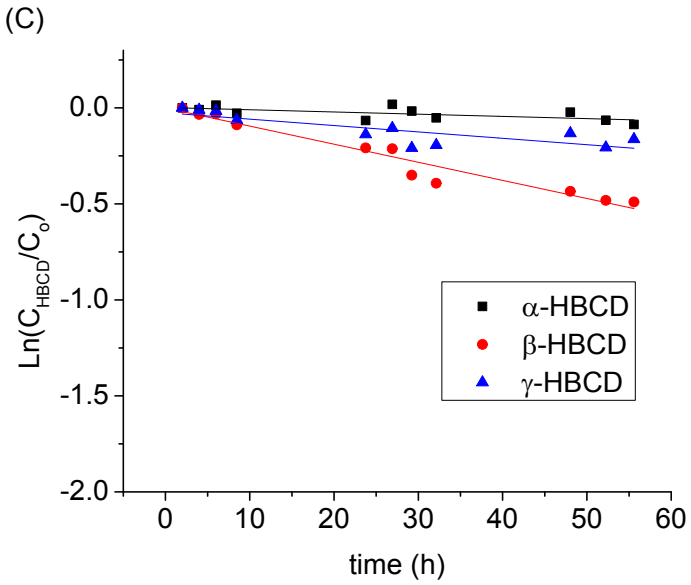

Fig. S6. Plot of $Ln(C_{HBCD}/C_0)$ versus time for the reaction of 1.0 μM HBCD in the presence of 2.5 mg mL^{-1} magnetite and an initial concentration of 6.0 mM Fe(II) at pH 7.0 with (A) 20 ppb PPHA; (B) 100 ppb PPHA; and (C) 200 ppb PPHA.

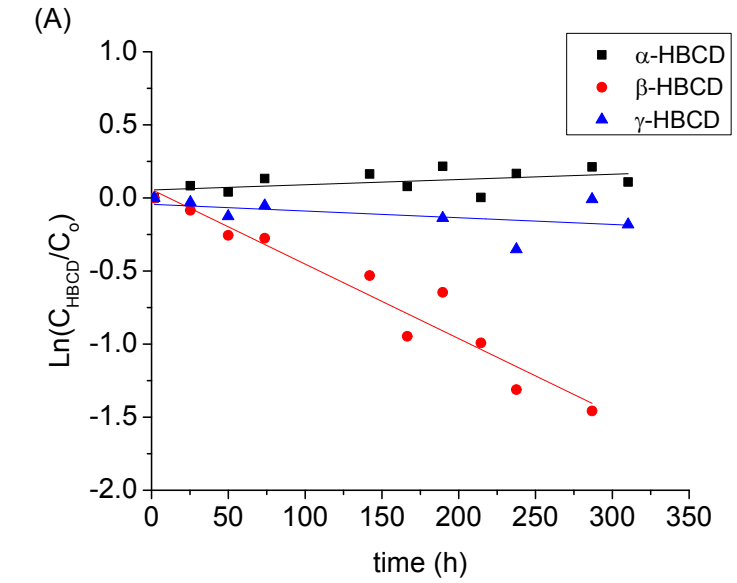
(A)
α-HBCD
β-HBCD
γ-HBCD
Ln(C_HBCD/C_o)
time (h)
1.0
0.5
0.0
-0.5
-1.0
-1.5
-2.0
0
50
100
150
200
250
300
350

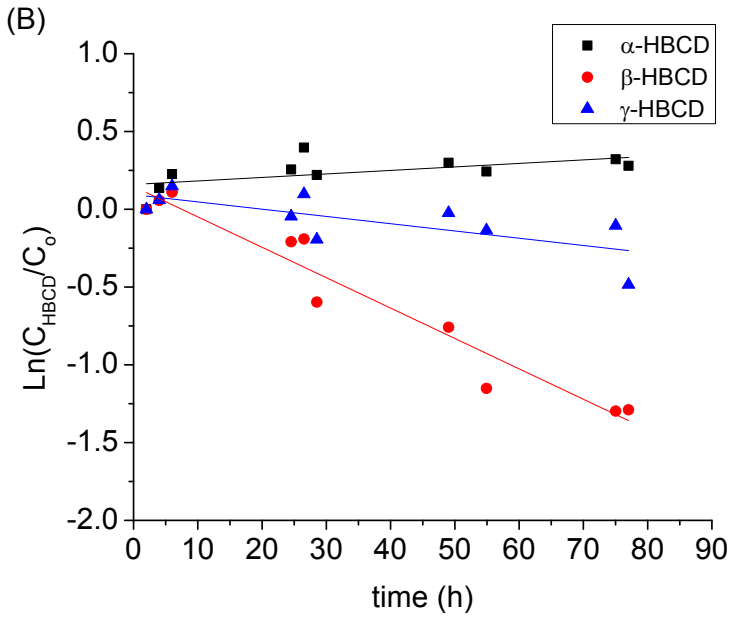
(B)
α-HBCD
β-HBCD
γ-HBCD
Ln(C_HBCD/C_o)
time (h)
1.0
0.5
0.0
-0.5
-1.0
-1.5
-2.0
0
10
20
30
40
50
60
70
80
90

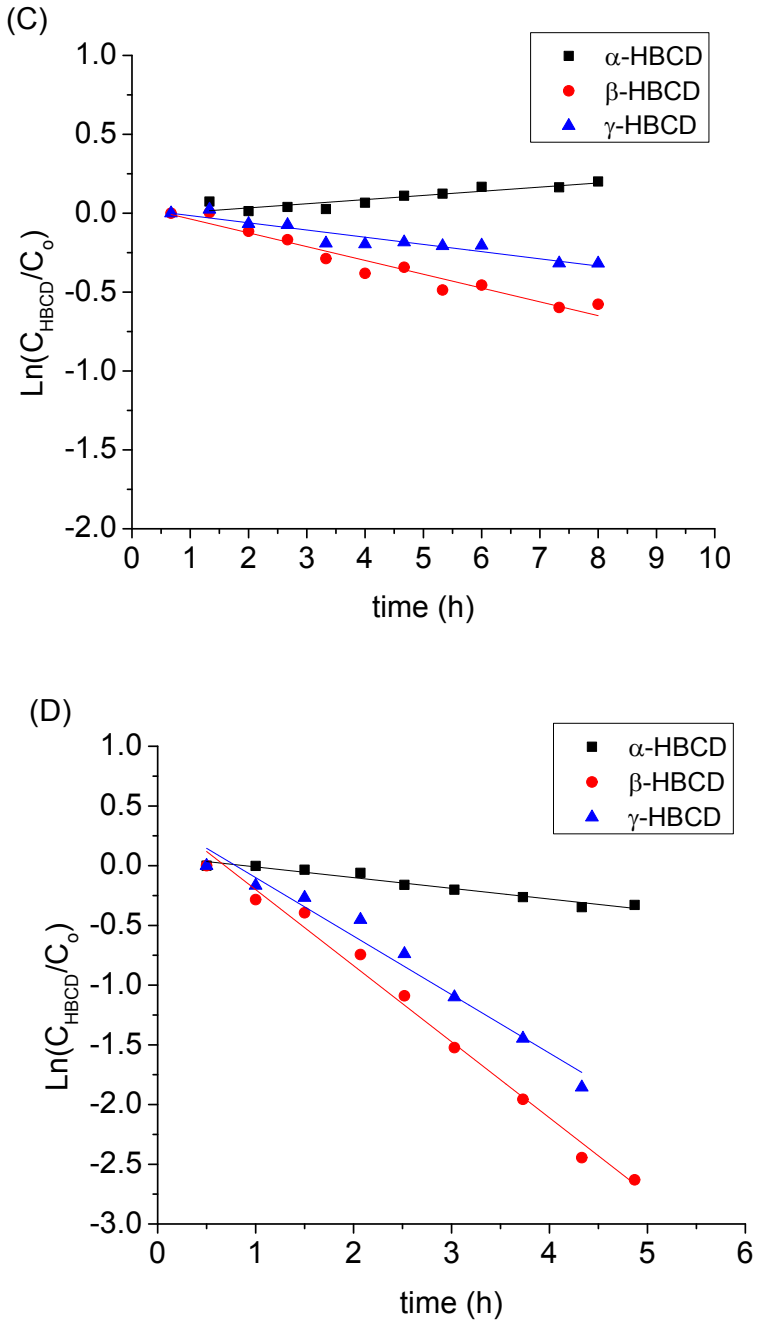

Fig. S7. Plot of $Ln(C_{HBCD}/C_0)$ versus time for the reaction of 1.0 µM HBCD in the presence of 5.0 mg mL^{-1} goethite and an initial concentration of 3.0 mM Fe(II) at (A) pH 6.16; (B) pH 6.76; (C) pH 7.12; and (D) pH 7.42.

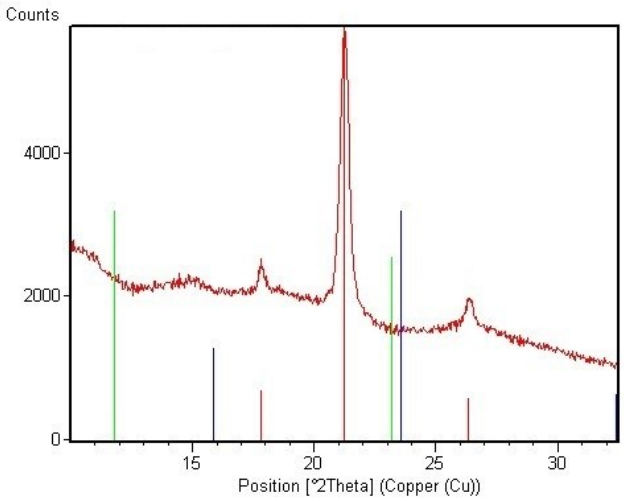

Fig. S8. The XRD pattern for goethite collected after the reaction of 1.0 μM HBCD in the presence of 5.0 mg mL^{-1} goethite and an initial concentration of 3.0 mM Fe(II) at pH 7.42.

The red lines indicate the peaks for goethite (reference code: 00-29-0713) while the green and blue lines indicate the peaks for green rust I (reference code: 00-13-0090) and green rust II (00-41-0014) in ICDD PDF4+ database, respectively.

Table S2. The concentration of sorbed Fe(II) and observed pseudo-first-order rate constants for the reaction of 1.0 μM HBCD in the presence of 5.0 mg mL^{-1} goethite and an initial concentration of 3.0 mM Fe(II) at various pH values

pH	7.42			7.12			6.76			6.16		
$Fe(II)_{sorbed}$ (mmol g^{-1})	0.09			0.19			0.12			0.04		
k_{obs} (h^{-1})	**total**	aqueous	solid	**total**	aqueous	solid	**total**	aqueous	solid	**total**	aqueous	solid
α-HBCD	**9.0(±1.7) ×10^{-2}**	6.8(±1.6) ×10^{-2}	1.1(±0.2) ×10^{-1}	**NA**	NA	NA	**NA**	NA	NA	**NA**	NA	NA
β-HBCD	**6.4(±0.6) ×10^{-1}**	6.1(±0.5) ×10^{-1}	6.5(±0.4) ×10^{-1}	**8.8(±1.6) ×10^{-2}**	1.0(±0.1) ×10^{-1}	8.2(±1.2) ×10^{-2}	**2.0(±0.4) ×10^{-2}**	1.4(±0.2) ×10^{-2}	2.3(±0.3) ×10^{-2}	**5.1(±1.1) ×10^{-3}**	4.5(±1.3) ×10^{-3}	5.5(±1.0) ×10^{-3}
γ-HBCD	**4.9(±0.8) ×10^{-1}**	7.5(±0.9) ×10^{-1}	4.5(±0.5) ×10^{-1}	**4.6(±1.1) ×10^{-2}**	1.2(±0.1) ×10^{-1}	3.1(±0.8) ×10^{-2}	**4.7(±3.6) ×10^{-3}**	1.1(±0.3) ×10^{-2}	3.2(±2.8) ×10^{-3}	**NA**	NA	NA

The uncertainties reflect the 95% confidence limit and it is reported as $t_{95\%}$ (t-value for 95% confidence limit) times standard deviation of slope in observed pseudo-first-order rate constant determination plot.
NA = Not Available, NA is presented in the table because the reactions are too slow and k_{obs} are smaller than their uncertainties.

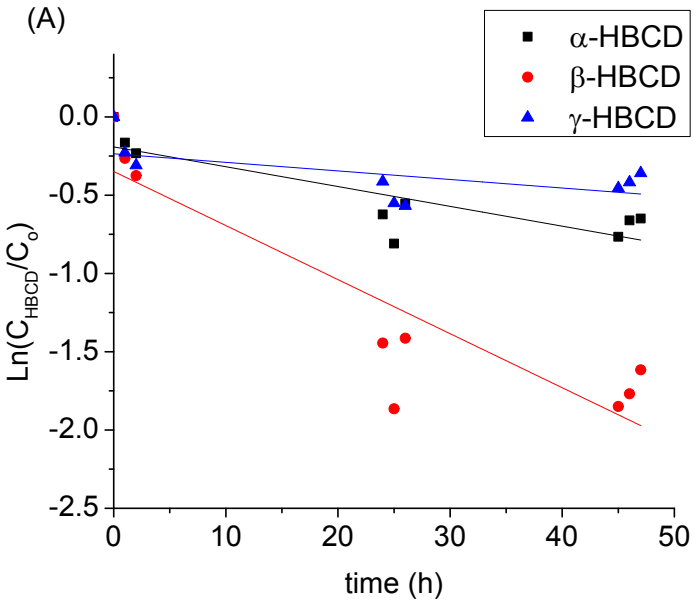
(A)
α-HBCD
β-HBCD
γ-HBCD
0.0
-0.5
-1.0
-1.5
-2.0
-2.5
0
10
20
30
40
50
time (h)
Ln(C_HBCD/C_o)

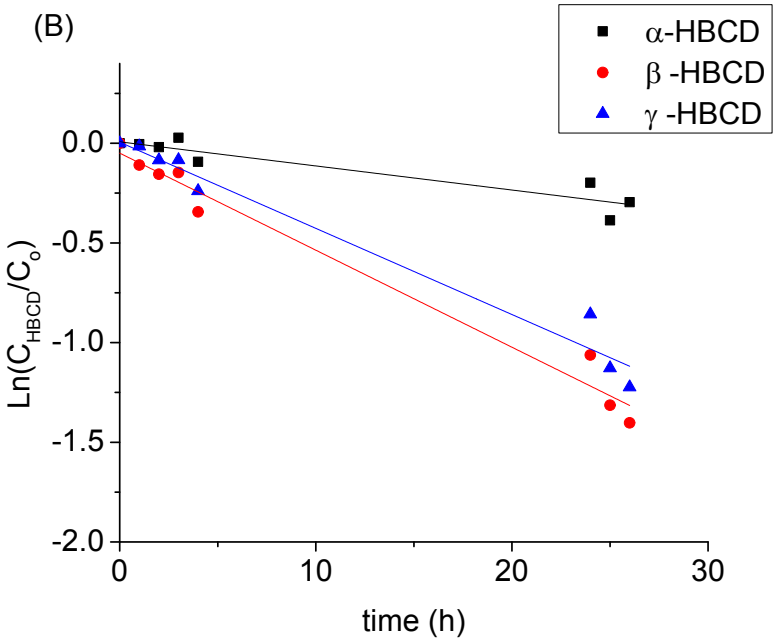
(B)
α-HBCD
β -HBCD
γ -HBCD
0.0
-0.5
-1.0
-1.5
-2.0
0
10
20
30
time (h)
Ln(C_HBCD/C_o)

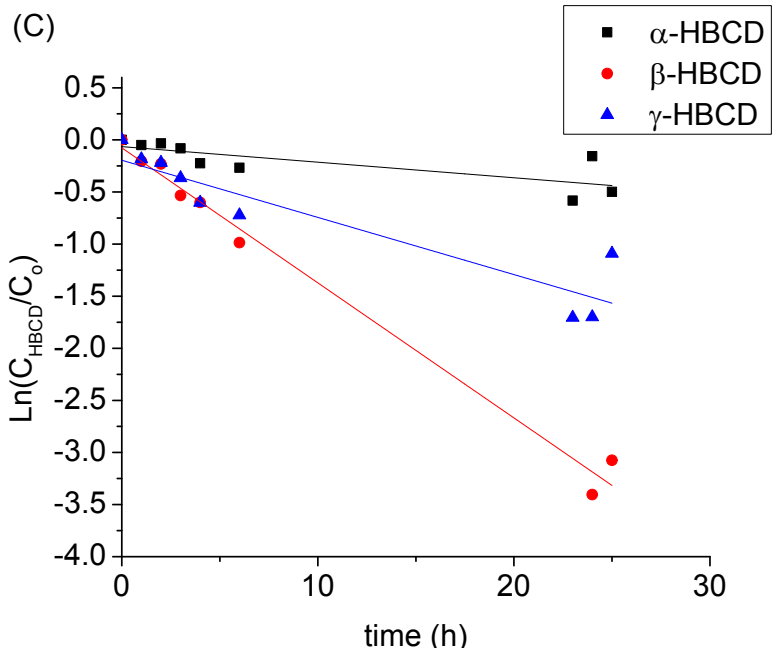

Fig. S9. Plot of $Ln(C_{HBCD}/C_0)$ versus time for the reaction of 1.0 μM HBCD in the presence of 20 mg mL^{-1} hematite and an initial concentration of 3.0 mM Fe(II) at (A) pH 6.85; (B) pH 6.95; and (C) pH 7.15.

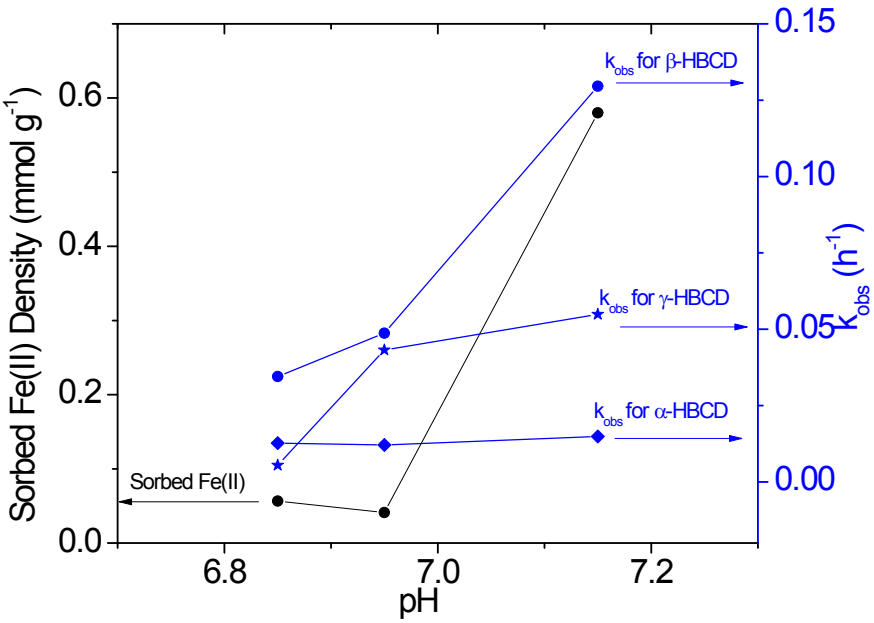

Fig. S10. Sorption of Fe(II) onto hematite (left axis) and observed pseudo-first-order rate constants for the reaction of HBCD (k_{obs}, right axis) in the presence of 20 mg mL^{-1} hematite and an initial concentration of 3.0 mM Fe(II) at various pH values.

Table S3. The concentration of sorbed Fe(II) and observed pseudo-first-order rate constants for the reaction of 1.0 µM HBCD in the presence of 20 mg mL^{-1} hematite and an initial concentration of 3.0 mM Fe(II) at various pH values

pH	7.15			6.95			6.85		
$Fe(II)_{sorbed}$ (mmol g^{-1})	0.058			0.041			0.056		
k_{obs} (h^{-1})	**total**	aqueous	solid	**total**	aqueous	solid	**total**	aqueous	solid
α-HBCD	**1.5(±1.1) ×10^{-2}**	7.8(±7.1) ×10^{-3}	1.9(±1.0) ×10^{-2}	**1.2(±0.5) ×10^{-2}**	1.1(±0.5) ×10^{-2}	1.3(±0.7) ×10^{-2}	**1.3(±0.7) ×10^{-2}**	5.6(±9.6) ×10^{-3}	2.2(±1.2) ×10^{-2}
β-HBCD	**1.3(±0.1) ×10^{-1}**	NA	1.3(±0.3) ×10^{-1}	**4.9(±0.7) ×10^{-2}**	4.4(±1.0) ×10^{-2}	5.0(±0.5) ×10^{-2}	**3.5(±1.5) ×10^{-2}**	2.6(±1.4) ×10^{-2}	3.9(±1.6) ×10^{-2}
γ-HBCD	**5.5(±2.0) ×10^{-2}**	NA	4.1(±1.1) ×10^{-2}	**4.3(±0.7) ×10^{-2}**	4.0(±1.2) ×10^{-2}	4.3(±0.7) ×10^{-2}	**5.5(±6.3) ×10^{-3}**	4.8(±2.1) ×10^{-2}	NA

The uncertainties reflect the 95% confidence limit and it is reported as $t_{95\%}$ (t-value for 95% confidence limit) times standard deviation of slope in observed pseudo-first-order rate constant determination plot.
NA = Not Available, NA is presented in the table because the reactions are too slow and k_{obs} are smaller than their uncertainties.

References

Sing, K.S.W., 1982. Reporting physisorption data for gas/solid systems with special reference to the determination of surface area and porosity (Provisional), Pure and Applied Chemistry, pp. 2201-2218.